Article ID: 1007-4627(2016) 02-0190-07

Projected Shell Model Description for the Proton Emitters

BIAN Bao'an(卞宝安)

(*School of Science, Jiangnan University, Wuxi 214122, Jiangsu, China*)

Abstract: Proton radioactivity is an important decay mode for nuclei near the proton drip-line. Studies of this decay mode can reveal valuable information on exotic nuclear structure and provide important information on the stucture of nuclei in extreme conditions. The new experimental data can let us understand the interactions in exotic systems, which motivate further theoretical development. The most recent application of the projected shell model (PSM) for proton emitters is represented. We study the rotational bands of the deformed proton emitter ^{141}Ho by using the PSM. The experimental data are well reproduced. Strongly suppressed γ transition from the low-lying $I^{\pi}= 3/2^{+}$ state makes this state isomeric. Variations in the dynamical moment of inertia are discussed due to band crossings using the band diagram. The calculated results for proton emitter ^{151}Lu shows it is oblately deformed.

Key words: proton emitter; nuclear deformation; rotational band; decay half-life

CLC number: O571.21 **Document code:** A **DOI:** 10.11804/NuclPhysRev.33.02.190

http://www.npr.ac.cn

1 Introduction

Studies of nuclei far from the line of β stability have become an important subject in nuclear structure studies[1−3]. The structure of nuclei near the drip lines may be different from that of nuclei along the valley of stability. The studies of structure and decay of exotic nuclei can test the present nuclear theory and model, and promote their development[4].

In the region of proton-rich nuclei far from the line of β stability, the nuclei with large proton excess can make the nuclear system stable through emitting proton, which is called proton radioactivity[5]. Proton radioactivity is an important decay mode of nuclei far from the line of β stability. Usually, proton emitter with lower Z near the drip line exist as a resonance state with short lifetime. While near the drip with high Z, the proton emitter with longer lifetime can be observed due to Coulomb interaction of unbound proton and core. In fact, the parent nucleus is in a quasistationary state, and the proton decay may be considered as a process where the proton tunnels through the potential barrier. The decay rate of proton emission is sensitive to parent and daughter nucleus, and the half-life offers the information of wave function of proton resonance. Experimental information on proton emitter offers a basis to understand the fundamental nuclear interactions near the drip lines. Theoretical calculations have predicted interesting modifications from the nuclear structure properties known for stable nuclei.

Advances in the experimental techniques[6−13] have allowed one to get deep insights into the organization of nuclei with extreme conditions. Proton radioactivity has been investigated from the spherical proton emitters in their ground states (for some cases from the isomeric state) between $Z = 69$ and $Z = 81$[7]. While the anomalous decay rates observed in recent experiment suggest a large deformation for the core[8]. The subsequent proton emission from ground state to 2^{+} state in the daughter nucleus in ^{131}Eu is observed[9]. With the development of technology, more proton emitters are observed[10−12]. The experimental results promote the study of proton decay theoretically, especially from deformed nuclei[13−16]. Generally, proton emission only involves the movement of one proton through the Coulomb barrier. But proton emission is complex actually. It is different to divide the wave function of nucleus into two parts with one proton and daughter nucleus. In addition, nuclear structure also affects the decay in proton emitter. While for spherical nuclei, many theories give the good results[17−18]. For example, the experimental half-lives are reproduced by half-life by the spherical WKB approximation and Born distorted-wave Born approximation (DWBA). The theoretical tools available for deformed

Received date: 11 Nov. 2015;

Foundation item: National Natural Science Foundation of China (11005050)

Biography: BIAN Bao'an(1979–), male, Lianyungang, Jiangsu, Associate Professor, working on nuclear physics; E-mail: baoanbian@jiangnan.edu.cn.

emitters are developed. In the framework of particle-rotor model, many methods are applied to study the proton emitters, such as adiabatic coupled-channel method with Gamow states[13,19], extended Bugrov-Kadmenskii method[8−9], noadiabatic coupled-channel method with Gamow states[14],coupled-channel description with Green′s function method[15] nonadiabatic quasiparticle method[20]. Other theories are relativistic Hartree-Bogoliubov model[21] and the approach based on the time-dependent schrödinger equation[22]. These studies can well describe the properties of the proton emitters, although not all of these are based on a fully microscopic and self-consistent description of proton unstable nuclei.

Most of the theoretical investigations have been focused on the discussion of half-lives of proton emission. There are not many theoretical works about nuclear structure of proton emitter. Recently, high-quality spectroscopic information of ground and isomeric state along the proton drip line have been observed experimentally, allowing us to understand the deformed proton emitters at higher spins. The in-beam spectroscopy for proton emitters was reported by Yu *et al.*[23] Rotational bands feeding the ground state and an isomeric state in the proton emitters ^{147}Tm and ^{141}Ho were observed[24−25], which indicate that these two nuclei are deformed. Rotational bands based on the $\pi h_{11/2}$ orbital in ^{145}Ho and ^{145}Tm were also reported[26−27], and the structure of proton unbound state along the proton drip line can be further understood. These experimental data can serve as an ideal testing ground for nuclear structure models that are applicable to the drip lines. The experimental data have an important impact on theories, which provide an ideal test case for nuclear structure models.

In our work, it is the first time for projected shell model (PSM) [28] to be used to investigate the structure of the proton emitter. The nucleus ^{141}Ho studied is known to have large deformation, which is an ideal case to test our theory[29]. And an middle deformed ^{151}Lu is also calculated.

2 Outline of the theory

A PSM calculation is carried out in the deformed Nilsson single-particle states[30]. Deformed states are defined in the intrinsic frame of reference where the rotational symmetry is broken. In order to calculate the observables, the broken rotational symmetry is restored in the wave functions. This can be completed by using the standard angular momentum projection method The projected states are then used to diagonalize a two-body shell model Hamiltonian. The difference from the conventional shell model is that calculation is performed in a deformed basis rather than a spherical one in PSM.

A deformed basis is constructed from the standard Nilsson model, and the parameters κ and μ in the Nilsson potential are taken from Ref. [31]. After a BCS calculation, the deformed quasiparticle (qp) states can be constructed, which are the starting point of the PSM. The set of multi-qp states for our shell model configuration space is

$$|\phi_\kappa\rangle = \{a_\pi^+|0\rangle, a_\pi^+ a_{\nu_1}^+ a_{\nu_2}^+|0\rangle\} \ , \tag{1}$$

where a^+s are the qp creation operators, $\pi s(\nu s)$ represent the proton (neutron) Nilsson quantum numbers which run over the low-lying orbitals, and $|0\rangle$ is the Nilsson + BCS vacuum (0-qp state). In Eq. (1), the 3-qp states selected for the many-body basis consist of the 1-qp proton state plus a pair of qps from neutrons.

The pairing plus quadrupole-quadrupole (QQ) Hamiltonian with the quadrupole-pairing term are included in the Hamiltonian[32]

$$\hat{H} = \hat{H}_0 - \frac{1}{2}\chi\sum_\mu \hat{Q}_\mu^+\hat{Q}_\mu - G_{\rm M}\hat{P}^+\hat{P} - G_{\rm Q}\sum_\mu \hat{P}_\mu^+\hat{P}_\mu \ , \tag{2}$$

where $\hat{H}_0$ is the spherical single-particle Hamiltonian, which includes a proper spinorbit force[31]. The second term in the Hamiltonian is Q-Q interaction and the last two terms are the monopole and quadrupole pairing interactions, respectively. The Q-Q interaction strength χ is ajusted such that the quadrupole deformation ε_2 is obtained from the self-consistent mean-field calculation[28]. The monopole pairing strength $G_{\rm Q}$ is expressed by $G_{\rm M} = [20.12 \mp 13.13(N-Z)/A]/A$, with "–" for neutrons and "+" for protons[28]. The quadrupole pairing strength $G_{\rm Q}$ is proportional to $G_{\rm M}$, and the proportionality constant is taken as 0.16 in the present work. Three major shells $N = 3, 4, 5$ are included for both neutrons and protons as the valence single-particle space.

Then the Hamiltonian in the shell model space spanned by $\hat{P}^I_{\rm MK}|\phi_\kappa\rangle$ is diagonalized. Thus the PSM wave function is given by

$$\Psi^\sigma_{\rm IM} = \sum_{KI,\kappa} f^\sigma_\kappa \hat{P}^I_{\rm MK}|\phi_\kappa\rangle \ , \tag{3}$$

where σ specifies the states with same angular momentum and κ represents the basis states. $\hat{P}^I_{\rm MK}$ is the angular momentum-projection operator. The set of eigenvalue equations for each spin I in the PSM are obtained by

$$\sum_{\kappa'}\{H_{\kappa\kappa'} - E_\sigma N_{\kappa\kappa'}\} f_{\kappa'\sigma} = 0 \ , \tag{4}$$

http://www.npr.ac.cn

The Hamiltonian matrix elements $H_{\kappa\kappa'}$ and the norm matrix elements $N_{\kappa\kappa'}$ are defined as

$$H_{\kappa\kappa'} = \langle\phi_\kappa|\,\hat{H}\hat{P}^I_{KK'}\,|\phi_\kappa\rangle \ , \quad N_{\kappa\kappa'} = \langle\phi_\kappa|\,\hat{P}^I_{KK'}\,|\phi_\kappa\rangle \ . \tag{5}$$

The expectation value of the Hamiltonian with a rotational band κ, $H_{\kappa\kappa'}/N_{\kappa\kappa'}$ defines a band energy. The band diagram[28] describes the band energies as functions of spin I. In a band diagram the bands with various configurations are shown before they are mixed by the diagonalization procedure of Eq. (4).

3 Results and discussion

The present PSM calculations are carried out for ^{141}Ho with deformation parameters $\varepsilon_2 = 0.258$ and $\varepsilon_4 = -0.035$, which are consistent with the values extracted from experiment[25]. The calculated energy levels for the negative-parity $7/2^-$ band and the positive-parity$1/2^+$ band are shown in Fig. 1. It can be seen that the experimental data are reproduced rather well by the calculation. The 1-qp proton configuration with K^π=$7/2^-$ built on the $h_{11/2}$ orbital is found to be the lowest in energy that defines the yrast sequence, which agrees with the results of Ref. [25]. On the other hand, the calculated 1-qp proton configuration with K^π=$1/2^+$ of $d_{3/2}$ is the lowest among all the positive-parity bands. An excitation energy of 66 keV is deduced for the isomeric $1/2^+$ state in the experiment; however, the band built on it was uncertain[25]. The present calculation shows that the positive-parity band built on the proton $1/2^+$ state has the bandhead energy of 49.8 keV, and the $3/2^+$ state lies 4 keV higher than the $1/2^+$ bandhead.

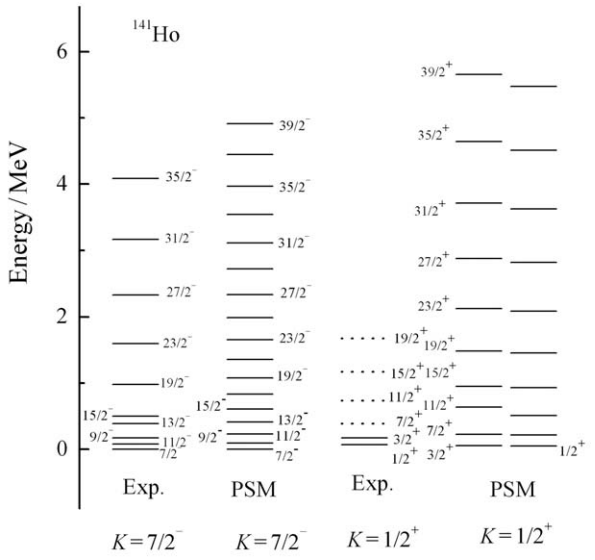

Fig. 1 Calculated energy levels for ^{141}Ho and comparison with experimental data. This figure is taken from Ref. [29].

The positive-parity $K^\pi = 1/2^+$ band exhibits an approximate pairwise degeneracy, as shown in the $E(I)$–$E(I–1)$ plot in Fig. 2(a). Because of the degeneracy, the energies $E(I)$ of this rotational band split into two branches of the $\Delta I = 2$ cascade (the so-called signature splitting[33]), one of which (with $I = 3/2,\ 7/2,\ \ldots$) is energetically favored and the other (with $I = 1/2,\ 5/2,\ \ldots$) is unfavored. Only the energetically favored branch can be observed experimentally[25]. Fig. 2(b) shows the calculated $B(M1, I \to I-1)$ values for this band. It can be seen that the M1 transition occurs only from the unfavored to the favored branch, while those from the favored to the unfavored branch are strongly suppressed. Especially, the negligible γ decay of $B(M1, 3/2^+ \to 1/2^+)$ makes the $3/2^+$ state isomeric and a proton emission could become the favorite decay mode for this state. This result is consist with the study with the nonadiabatic quasiparticle model[34] that suggested that the isomeric state from which the proton is emitted is the $3/2^+$ state, not the $1/2^+$ bandhead.

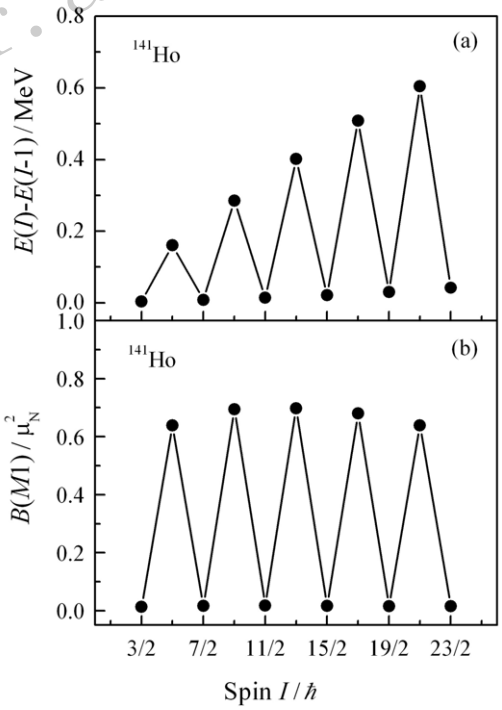

Fig. 2 (a) Calculated energy differences between spin states I and $I-1$ for the positive-parity $K^\pi = 1/2^+$ band, and (b) $B(M1, I \to I-1)$ values for this band. This figure is taken from Ref. [29].

The moment of inertia in deformed nuclei is helpful to investigate the rotational behavior. In Fig. 3, we display the calculated dynamical moment of inertia $J^{(2)}$ and available data. The dynamical moment of inertia of a band is defined by

http://www.npr.ac.cn

$$J^{(2)} = \frac{4}{E_\gamma(I) - E_\gamma(I-2)} \ , \tag{6}$$

where the transition energy $E_\gamma = E(I) - E(I-2)$, and the rotational frequency by

$$\hbar\omega = \frac{E_\gamma}{\sqrt{(I+1)(I+2)-K^2} - \sqrt{(I-1)I-K^2}} \ . \tag{7}$$

It is can be seen in Fig. 3(a) that the experimental $J^{(2)}$of the $7/2^-$ band shows a smooth rise up to $\hbar\omega \approx 0.3$ MeV as rotational frequency increases and then increases more rapidly. The observed behavior for $J^{(2)}$ is well reproduced by the our calculation. The present calculation further predicts a turning back in $J^{(2)}$. Due to limited experimental data for the $1/2^+$ band, so the discussion for this band is mainly a prediction. One can see in Fig. 3(b), the PSM reproduces the observed dramatic change of $J^{(2)}$ at low rotational frequencies and further predicts another rise at $\hbar\omega \approx 0.32$ MeV. $J^{(2)}$ shows a zigzag behavior for the high-spin states of the $1/2^+$ band, which needs future experimental confirmation.

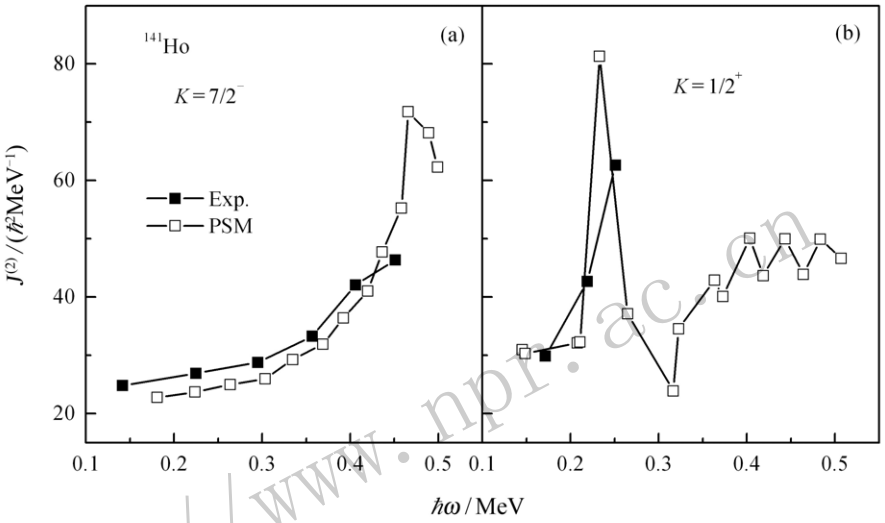

Fig. 3　Calculated dynamical moments of inertia for ^{141}Ho and comparison with available experimental data. This figure is taken from Ref. [29].

http://www.npr.ac.cn

Variation of $J^{(2)}$ is an important indication for structure changes in wave functions. It is interesting to study the details of what particular orbitals contribute to the changes of $J^{(2)}$. In PSM, band crossings between bands of 1- and 3-qp configurations can describe changes in rotational behavior in odd-mass nuclei through plotting band diagrams. In Fig. 4, the relevant 1- and 3-qp bands are displayed in ^{141}Ho, whose corresponding configuratons are represented. For the negative-parity bands in Fig. 4(a), one can see that the 1-qp $K = 7/2$ band goes monotonically up, obeying approximately the $E \sim I(I+1)$ rule for a rotor. This suggests that this band is strongly coupled to the rotating body. However, it is approached by several other bands when spin increases. Due to the band interaction, the regular behavior of the $K = 7/2$ band is disturbed. The 1-qp $K = 5/2$ band with a smaller slop comes closer to the $K = 7/2$ band in the intermediate spin region. The interaction of this band with the $K = 7/2$ one results in a change of $J^{(2)}$, making it rise more rapidly. A band crossing is observed at about $I = 37/2$, where a 3-qp band crosses the 1-qp $K = 7/2$ band. The crossing 3-qp band has the configuration of the $\pi(K = 7/2, h_{11/2})$ proton coupled to a pair of neutronsof $\nu[(K = 7/2, h_{11/2}) + (K = 1/2, f_{7/2})]$. The band crossing results in significant changes of the yrast structure and a sharp peak occurs in $J^{(2)}$ at $\hbar\omega \approx 0.47$ MeV, as shown in Fig. 3(a). The lowest positive-parity band mainly comes from the $K = 1/2$ state of the proton $d_{3/2}$ orbital. While this configuration is strongly disturbed by another nearby one with $K = 7/2$ of the proton $g_{7/2}$ orbital at spin $I = 7/2$ as shown in Fig. 4(b). The interaction between them causes irregularity at very low rotational frequencies around $\hbar\omega \approx 0.25$ MeV, as seen in Fig. 3(b). It is also observed in Fig. 3(b) that the behavior of the $K = 1/2$ band becomes more regular with increase of spin, exhibiting a zigzag behavior because of the low-Kcharacter of the configuration. At higher spins, some 3-qp bands is close to the $K = 1/2$ 1-qp band. The 3-qp bands are composed of the proton $\pi(K = 7/2, g_{7/2})$ or $\pi(K = 1/2, d_{3/2})$ coupled to a pair of neutrons $\nu[(K = 7/2, h_{11/2}) + (K = 1/2, f_{7/2})]$.

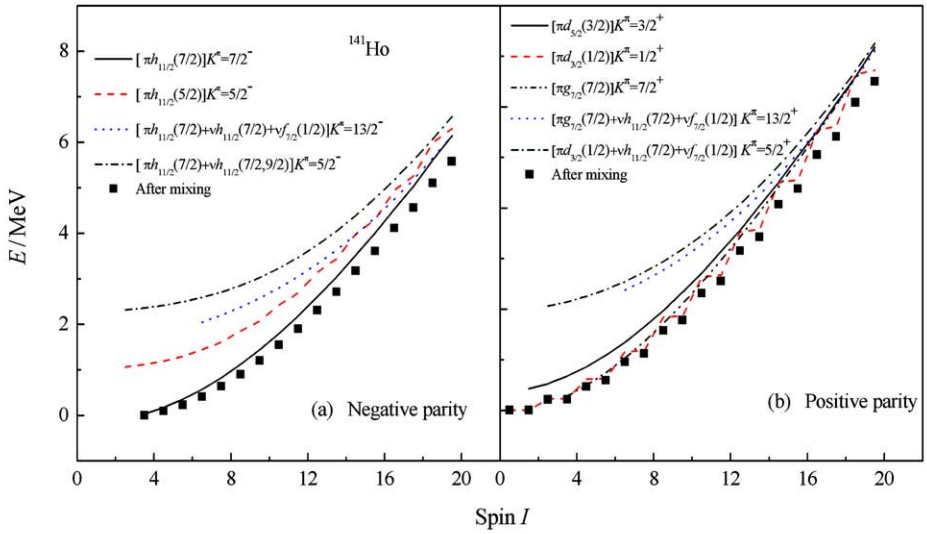

Fig. 4 (color online) Calculated band diagrams for ^{141}Ho. This figure is taken from Ref. [29].

It is known that hexadecapole deformation can modify the single-particle states generated by the usual quadrupole-deformed potential. For ^{141}Ho, the two low-Kproton single-particle states, $\pi(K=1/2,d_{3/2})$ and $\pi(K=3/2,d_{5/2})$, approach the proton Fermi surface, therefore, both could have a chance to be the lowest positive-parity configuration. Our calculations suggest that their positions depend sensitively on the degree of hexadecapole deformation. The present result is consistent with the conclusion of Ref. [25] that ^{141}Ho has significant hexadecapole deformation near the ground state.

We perform the calculations for proton emitter ^{151}Lu to further test our model. Fig. 5 shows the calculated energy levels for the negative-parity and positive-parity bands for ^{151}Lu, together with the experimental data[35−36]. The calculations are performed for ^{151}Lu with deformation parameters $\varepsilon_2=-0.141,\varepsilon_4=-0.04$. This indicates that ^{151}Lu is oblate nucleus, which is consistent with the nonadiabatic quasiparticle calculations that suggest an oblately deformed, $11/2^-$ and $3/2^+$ proton-emitting states with a quadrupole deformation of $\beta_2=-0.11$[35] and $-0.11^{+0.02}_{-0.05}$[36], respectively. One can see that the data are reproduced well at low spins by the present calculations. The calculated energy levels of $23/2^-$ and $27/2^-$ are almost degenerated, which results from the bands interaction. The further experiments are necessary to confirm the energies predicted at high spins.

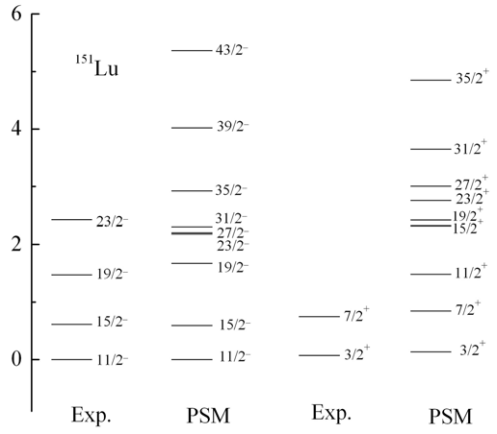

Fig. 5 Calculated energy levels for ^{151}Lu and comparison with experimental data.

To understand the information of nuclear structure, in Fig. 6. we plot the relevant 1- and 3-qp bands in ^{151}Lu for negative parity and positive parity, whose configurations are given in the figure. For negative parity, the $K^\pi=5/2^-$ band is close to the $K^\pi=3/2^-$, there is a competitive relationship. The 1-qp proton configuration with $K^\pi=3/2^-$ from the $h_{11/2}$ orbital is found to be the lowest in energy at low spins. It suggests that the ground of an oblate nucleus is $K^\pi=3/2^-$, while the result of Re[37] suggests a ground state of $K^\pi=5/2^-$. The energies of 3-qp bands at high spins are lower than the 1-qp bands. Therefore, the ground band at high spin is composed of the 3-qp configuration. The 3-qp band with $K^\pi=5/2^-$ comes close to other two 3-qp bands, the interaction between them leads to irregularity of energy at $I=27/2$. For positive parity, the calculated 1-qp proton configuration with $K^\pi=3/2^+$of $d_{3/2}$ is the lowest at low spins，suggesting that the isomeric state of ^{151}Lu comes from $K^\pi=3/2^+$ that is in agreement with the suggestion Ref. [37]. While energies of the 3-qp bands at high spins are lower than the 1-qp bands. Thus, the 3-qp configurations contribute

http://www.npr.ac.cn

to the $3/2^+$ band at high spins. Meanwhile, The 3-qp band with $K^\pi=7/2^+$ comes close to 3-qp band with $K^\pi=3/2^+$, whose interaction results in the irregularity of energy at $I=19/2$.

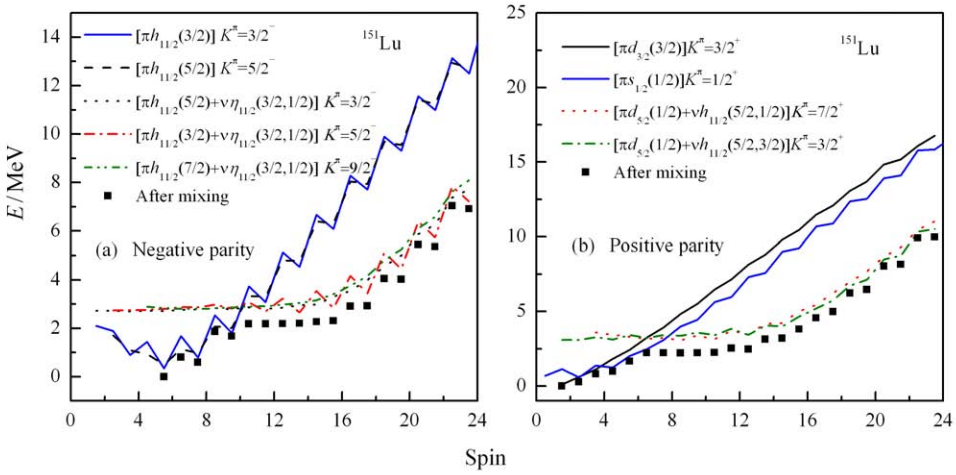

Fig. 6　(color online) Calculated band diagrams for ^{151}Lu.

4 Summary

The PSM has been applied to study the proton emitters successfully. A detailed calculation for the rotational bands in ^{141}Ho is performed using the PSM. We found that the calculation well describes the experimental data of the rotational band energies. One can find that strongly suppressed γ transitions from the low-lying $3/2^+$ state makes this state isomeric, in favor of the suggestion that a proton emission could become the favorite decay mode for this state. The variations in moments of inertia have been discussed according to various band crossings in the band diagram. The calculated energy for proton emitter ^{151}Lu is well reproduced, showing that this nucleus is oblately deformed.

The success of the PSM calculation for proton emitters suggests that the existing theoretical models may not need to consider significant modifications in order to describe the structure at the proton drip line in contrast to the neutron-rich side. This may result from the fact that these nuclei that lie at the proton-rich region are not very far from the β stable line, and the known concepts for the structure discussion are still applicable.

http://www.npr.ac.cn

References:

[1] REN Z Z, CHEN B Q, MA Z Y, *et al.* Phys Rev C, 1996, **53**: R572.

[2] MENG J, RING P. Phys Rev Lett, 1996, **77**: 3963.

[3] BLANK B, BORGE M J G. Prog Part Nucl Phys, 2008, **60**: 403.

[4] PFÜTZNER M, KARNY M, GRIGORENKO L V, *et al.* Rev Mod Phys, 2012, **84**: 567.

[5] WOODS P J, DAVIDS C N. Annu Rev Nucl Part Sci, 1997, **47**: 541.

[6] BINGHAM C R, TANTAWY M N, BATCHELDER J C, *et al.* Nucl Instr Meth B, 2005, **241**: 185.

[7] DAVIDS C N, WOODS P J, BATCHELDER J C, *et al.* Phys Rev C, 1997, **55**: 2255.

[8] DAVIDS C N, WOODS P J, SEWERYNIAK D. Phys Rev Lett, 1998, **80**: 1849.

[9] SONZOGNI A A, DAVIDS C N, WOODS P J, *et al.* Phys Rev Lett, 1999, **83**: 1116.

[10] BINGHAM C R, BATCHELDER J C, RYKACZEWSKI K, *et al.* Phys Rev C, 1999, **59**: R2984.

[11] SORAMEL F, GUGLIELMETTI A, STROE L, *et al.* Phys Rev C, 2001, **63**: R031304.

[12] KETTUNEN H, ENQVIST T, GRAHN T, *et al.* Phys Rev C, 2004, **69**: 054323.

[13] FERREIRA L S, MAGLIONE E, LIOTTA R J. Phys Rev Lett, 1997, **78**: 1640.

[14] KRUPPA A T, BARMORE B, NAZAREWICZ W, *et al.* Phys Rev Lett, 2000, **84**: 4549.

[15] ESBENSEN H, DAVIDS C N. Phys Rev C, 2000, **63**: 014315.

[16] DELION D S, LIOTTA R J, WYSS R. Phys Rev Lett, 2006, **96**: 072501.

[17] ÅBERG S, SEMMES P B, NAZAREWICZ W. Phys Rev C, 1997, **56**: 1762.

[18] DAVIDS C N, ESBENSEN H. Phys Rev C, 2000, **61**: 054302.

[19] MAGLIONE E, FERREIRA L S, LIOTTA R J. Phys Rev Lett, 1998, **81**: 538.

[20] FIORIN G, MAGLIONE E, FERREIRA L S. Phys Rev C, 2003, **67**: 054302.

[21] VRETENAR D, LALAZISSIS G A, RING P. Phys Rev Lett, 1999, **82**: 4595.

[22] TALOU P, CARJAN N, STROTTMAN D. Phys Rev C,

1998, **58**: 3280.
[23] YU C H, BATCHELDER J C, BINGHAM C R, *et al*. Phys Rev C, 1998, **58**: R3042.
[24] SEWERYNIAK D, DAVIDS C N, WALTERS W B, *et al*. Phys Rev C, 1997, **55**: R2137.
[25] SEWERYNIAK D, WOODS P J, RESSLER J J, *et al*. Phys Rev Lett, 2001, **86**: 1458.
[26] GOETTIG L, GELLETLY W, LISTER C J, *et al*. Nucl Phys A, 1987, **475**: 569.
[27] SEWERYNIAK D, BLANK B, CARPENTER M P, *et al*. Phys Rev Lett, 2007, **99**: 082502.
[28] HARA K, SUN Y. Int J Mod Phys E, 1995, **4**: 637.
[29] BIAN B A, SUN Y, YANG Y C. Phys Rev C, 2014, **89**: 014317.
[30] NILSSON S G, TSANG C F, SOBICZEWSKI A, *et al*. Nucl Phys A, 1969, **131**: 1.
[31] ZHANG J Y, XU N, FOSSAN D, *et al*. Phys Rev C, 1989, **39**: 714.
[32] PETRACHE C M, SUN Y, BAZZACCO D, *et al*. Phys Rev C, 1996, **53**: R2581.
[33] SUN Y, FENG D H, WEN S X. Phys Rev C, 1994, **50**: 2351.
[34] ARUMUGAM P, FERREIRA L S, MAGLIONE E. Phys Lett B, 2009, **680**: 443
[35] TAYLOR M J, CULLEN D M, PROCTER M G, *et al*. Phys Rev C, 2015, **91**: 044322
[36] PROCTER M G, CULLEN D M, TAYLOR M J, *et al*. Phys Lett B, 2015, **725**: 79
[37] FERREIRA L S, MAGLIONE E. Phys Rev C, 2000, **61**: 021304.

http://www.npr.ac.cn